Iron-carbon bond lengths in carbonmonoxy and cyanomet complexes of the monomeric hemoglobin III from *Chironomus thummi thummi*: A critical comparison between resonance Raman and x-ray diffraction studies

(Raman scattering/carbon monoxide/cyanide/ligand geometry/insect hemoglobin)

NAI-TENG YU[†‡§], BOJAN BENKO[†‡¶], ELLEN A. KERR[†‡], AND KLAUS GERSONDE[‖§]

†School of Chemistry, Georgia Institute of Technology, Atlanta, GA 30332; and ‡Department of Ophthalmology, Emory University School of Medicine, Atlanta, GA 30322; and ‖Abteilung Physiologische Chemie, Rheinisch-Westfälische Technische Hochschule, D-5100 Aachen, Federal Republic of Germany

ABSTRACT   Soret-excited resonance Raman spectroscopy yields direct information regarding the iron-carbon bonding interactions in the cyanomet and carbonmonoxy complexes of hemoglobin III from *Chironomus thummi thummi* (CTT III) in solution. By isotope exchange in cyanide ($^{13}CN^-$, $C^{15}N^-$, and $^{13}C^{15}N^-$) and carbon monoxide (^{13}CO, $C^{18}O$, and $^{13}C^{18}O$), we have assigned the Fe(III)—CN$^-$ stretching at 453 cm^{-1}, the Fe(III)—C—N$^-$ bending at 412 cm^{-1}, the Fe(II)—CO stretching at 500 cm^{-1}, the Fe(II)—C—O bending at 574 cm^{-1}, and the C—O stretching at 1960 cm^{-1}. The resonance Raman data, in conjunction with those obtained from heme model complexes with well-known Fe—C bond distances, strongly suggest that the Fe(III)—CN$^-$ bond ($\approx$1.91 Å) is longer (hence weaker) than the Fe(II)—CO bond ($\approx$1.80 Å). This result disagrees with those of x-ray crystallographic studies [Steigemann, W. & Weber, E. (1979) *J. Mol. Biol.* 127, 309–338] in which the Fe—C bond lengths were reported as 2.2 Å in cyanomet and 2.4 Å in carbonmonoxy CTT III. Based on Badger's rule and normal mode calculations, the x-ray data would lead to the prediction of 279 cm^{-1} for the Fe(II)—CO stretching frequency in CTT III·CO, which was not observed. On the other hand, we estimate the Fe—CO bond as $\approx$1.82 Å, which is very similar to the 1.80-Å value in human Hb·CO crystals. Furthermore, we have used isotope shift data to estimate the Fe—C—O angle as 169 ± 5°, somewhat larger than the 161° value found by Steigemann and Weber. We therefore conclude that there must be errors in the x-ray crystallographic refinement for the ligand geometry in carbonmonoxy and cyanomet CTT III.

The hemoglobin from insect larvae of *Chironomus thummi thummi* (CTT III) is an interesting model system for understanding the mechanisms of protein control of heme reactivity (1–12). It is a monomeric allosteric hemoglobin exhibiting a Bohr effect, which can be correlated with a conformational transition (t→r) controlled by a single proton, as shown by ESR (2–6) and NMR (3, 7–12) studies. This allosteric conformational transition and the ligand affinity are modulated by the *trans* effect of the proximal histidine, the direct interaction of the exogenous ligand with its microenvironment, the protein–porphyrin interactions, and the electronic structure of the heme iron (1, 5). It has been demonstrated (3, 7, 13, 14) that the amplitude of the Bohr-effect curve, a measure of the interaction energy between the Bohr-proton binding site and the ligand binding site, depends on the nature of the exogenous ligand. The Bohr effect is largest for O_2 and smallest for CO and CN$^-$ binding.

Carbon monoxide (15, 16) and cyanide (17) bind to simple iron hemes in a linear fashion along the heme normal. In hemoglobins, an amino acid side chain on the distal side (in CTT III, it is the isoleucine E11) can cause restrictions on the ligand binding resulting in modified Fe—C—O or Fe—C—N groupings. X-ray structural refinements at 1.4-Å resolution by Steigemann and Weber (18) have described unusual Fe-ligand bond lengths and bond angles for carbonmonoxy and cyanomet CTT III in crystals. A bound ligand can force both the porphyrin system and the hindering distal amino acid group to change their positions so that the whole ligand–heme–protein system again reaches an energy minimum. In contrast to a ligand–heme model system, the structure of liganded hemoglobin is extremely sensitive to temperature and electrostatic interaction (variations in salt concentration and pH). Bond length and binding geometry may therefore be sensitive indicators of the actual state of the ligand–heme–protein interactions in hemoglobins. Since the numerous conformations of this system may be removed in a crystal, one needs more information about these subtle interactions in solution and under physiological conditions. At present, there is evidence that the fine-structure of CTT III in solution is not the same as it is in crystals. By proton NMR in solution (8, 19), CTT III has been shown to exist in two forms, which differ in heme orientation, related by an $\approx$180° rotation about the α,γ-meso axis at least in the metHbCN form. Only one component has been observed in the crystal state (18). Furthermore, the ^{15}N NMR data obtained from cyanide-ligated met CTT III are inconsistent with the x-ray data, which indicated two equally probable positions for the histidine E7. One conformation has the histidine E7 expelled from the pocket by isoleucine E11, while another has this histidine inside the heme pocket. The ^{15}N NMR studies in solution excluded any distal histidine–cyanide interaction in CTT III (20).

We felt, therefore, that it is necessary to have further information from other spectroscopic methods, especially from resonance Raman spectroscopy, which is capable of providing direct information on the nature of iron-ligand bonds in hemoproteins (ref. 21 and references cited therein). The multiple ligand-isotope labeling technique allows one to distinguish between iron-ligand stretching and bending vibrations (21–25). Through use of the x-ray structural data of heme model complexes, we establish a relation between

equilibrium Fe-ligand bond length and bond stretching force constant (Badger's rule). From resonance Raman data, in conjunction with Badger's rule, normal mode analysis, and ligand isotope shift, we deduce the iron-ligand bond length and the ligand bending angle in carbonmonoxy hemoglobin CTT III. Large discrepancies are found to exist between these resonance Raman results (solution) and x-ray structural data (crystals) of carbonmonoxy- and cyanomet CTT III (18). Finally, we believe that the solution parameters by resonance Raman spectra should be good indicators for changes in ligand strength and ligand geometry associated with allosteric transitions.

MATERIALS AND METHODS

The monomeric CTT III was separated from the dimeric components by gel filtration (2) and purified by ion exchange chromatography (5, 7); the procedures have recently been described in detail (26). The chemical homogeneity of CTT III was checked by 10% polyacrylamide gel disk-electrophoresis (pH 9.5). The R_f value was 0.60. The lyophilized salt-free protein was stored at $-30°C$.

Samples of cyanomet CTT III were prepared by first centrifuging and filtering ≈ 80 μM heme solutions (in 0.05 M Tris·HCl, pH 8.1). Buffered potassium cyanide solution was then added to form cyanomet CTT III. The isotope-substituted complexes were prepared similarly using $K^{13}CN$ (isotope enrichment, 90.6% ^{13}C), $KC^{15}N$ (95.2 atom % ^{15}N), and $K^{13}C^{15}N$ (90 atom % ^{13}C; 92 atom % ^{15}N).

Samples of carbonmonoxy CTT III were prepared by deoxygenating filtered protein solutions, introducing ≈ 1 atmosphere (1 atm = 101.3 kPa) of carbon monoxide, and reducing with buffered sodium dithionite solution. The complexes with carbon monoxide isotopes were prepared in a similar manner using ^{13}CO (Stohler Isotope Chemicals, Waltham, MA; 99 atom % ^{13}C), $C^{18}O$ (Stohler Isotope Chemicals; 99 atom % ^{18}O), and $^{13}C^{18}O$ (Prochem US Services, Summit, NJ; 91.7 atom % ^{13}C and 98.5 atom % ^{18}O), each at an initial pressure of 1 atm.

Iron(III) meso-tetraphenylporphyrin (TPP) bromide and iron(III)-μ-oxo-dimer deuteroporphyrin dimethyl ester [later treated with HCl(g) to convert it to the corresponding monomer] were purchased from Midcentury (Posen, IL). The CO complexes of these hemes (≈ 110 μM) were prepared in a manner similar to that described (24). The Fe(II)-TPP-pyridine-CO complex was prepared with pyridine (Py) (≈ 1.7 mM) as axial base in a benzene solution and Fe(II)-deuteroporphyrin dimethyl ester (deut)-tetrahydrofuran (H_4furan)-CO was prepared in pure tetrahydrofuran.

Resonance Raman spectra were obtained using a multichannel system equipped with dry-ice-cooled ($-62°C$) intensified silicon-intensified target vidicon detector (Princeton Applied Research Model 1254). It has an enhanced detection capability for weak Raman signals (27). The experiments used a Spectra Physics (Mountain View, CA) model 171 krypton ion laser. The 406.7 nm line was used for excitation of the CO complexes, and the 413.1 nm line was used for the CN^- complexes. Laser power at the sample was maintained at ≈ 10 mW. The sample in the rotating cell was spun throughout the measurements to avoid local heating and to decrease photodissociation. Raman spectra were collected at room temperature and by a 90°-scattering geometry. All spectra were calibrated using standard compounds. Reported wavenumbers are accurate to ± 1 cm^{-1} for sharp lines and to ± 2 cm^{-1} for broad lines.

RESULTS

Assignment of Fe(III)—CN$^-$ Stretching and Fe(III)—C—N$^-$ Bending Vibrations by Isotope Exchange. Fig. 1 displays the effect of cyanide isotope substitution on the resonance Ra-

man spectrum (310–550 cm^{-1}) of cyanomet CTT III excited at 413.1 nm. Two isotope-sensitive lines have been identified at 453 and 412 cm^{-1}. The line at 453 cm^{-1} shifts to 450 ($^{13}C^{14}N^-$), 450 ($^{12}C^{15}N^-$), and 446 cm^{-1} ($^{13}C^{15}N^-$). The same frequency at 450 cm^{-1} for both, the $^{13}C^{14}N^-$ and the $^{12}C^{15}N^-$ ligated forms, indicates that this vibrational frequency depends on the combined mass of cyanide, irrespective of the position of the isotope labeling. The $^{12}C^{15}N^-$ minus $^{13}C^{14}N^-$ difference spectrum [denoted in Fig. 1 as (c)−(b)] exhibits a complete cancellation near 450 cm^{-1}. This isotope behavior clearly indicates that the 453 cm^{-1} line is the ν[Fe(III)—CN$^-$] stretching mode, and the Fe(III)—C—N$^-$ linkage is essentially linear ($\theta > 170°$). The line at 412 cm^{-1} is somewhat complex because of the overlap by two vibrations: it becomes a doublet (at 403 and 414 cm^{-1}) for both the $^{13}C^{14}N^-$ and $^{13}C^{15}N^-$-ligated forms. However, the $^{12}C^{14}N^-$ and $^{12}C^{15}N^-$ behavior is indicative of the existence of two unresolved vibrational modes at 412 cm^{-1} (isotope sensitive) and 414 cm^{-1} (isotope insensitive). The isotope-sensitive component at 412 cm^{-1} is assigned to the δ[Fe(III)—C—N$^-$] bending mode because it exhibits decrease–increase–decrease zigzag isotope shifts from 412 $\rightarrow$ 403 $\rightarrow$ 412 $\rightarrow$ 403 cm^{-1} in the following order: $^{12}C^{14}N^- \rightarrow$ $^{13}C^{14}N^- \rightarrow$ $^{12}C^{15}N^- \rightarrow$ $^{13}C^{15}N^-$.

The isotope-insensitive component at 414 cm^{-1} may be assigned to the vinyl group bending vibration $\delta(C_bC_\alpha C_\beta)$ on the basis of recent work by Choi *et al.* (28) and Rousseau *et al.* (29). This assignment is supported by the studies on deutero cyanomet CTT III where the vinyl group bending at 414 cm^{-1} disappears and an isotope-sensitive line at 410 cm^{-1} exhibits zigzag isotope shifts (unpublished results).

The ν[Fe(III)—CN$^-$] vibration in carp cyanometHb was identified at 455 cm^{-1} via $C^{15}N^-$ isotope by Tsubaki and Yu (unpublished results cited in ref. 22) and at 452 cm^{-1} in human cyanometHb by Rousseau and co-workers (30, 31). However, no assignment of the δ[Fe(III)—C—N$^-$]bending
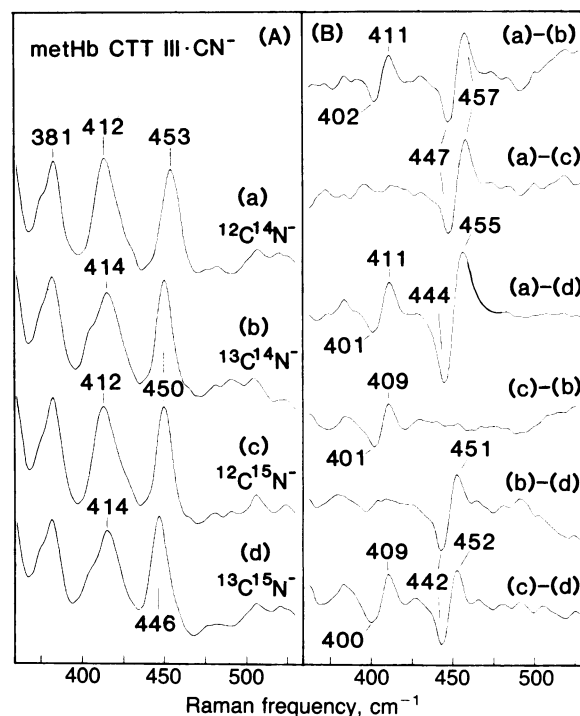

FIG. 1. CN$^-$ isotope effects on resonance Raman spectra (360–550 cm^{-1}) of cyanomet CTT III. Excitation wavelength λ, 413.1 nm; power, 15 mW; delay cycles, 10,000 (303 sec); slit width, 100 μm; in 50 mM Tris·HCl (pH 8.1). (*A*) Observed spectra with isotopes ($^{12}C^{14}N^-$, $^{13}C^{14}N$, $^{12}C^{15}N$, and $^{13}C^{15}N^-$. (*B*) Difference spectra between various ligand isotopes.

mode has been reported. Although attempts have been ma/kede, we have not been able to enhance the bound C—N stretching mode expected at ≈2130 cm⁻¹.

Assignment of Fe(II)—CO Stretching, Fe(II)—C—O Bending and C—O Stretching Vibrations by Isotope Exchange. In Fig. 2, we present resonance Raman spectra (200–650 cm⁻¹) of carbonmonoxy CTT III with various isotopes ($^{12}C^{16}O$, $^{13}C^{16}O$, $^{12}C^{18}O$, $^{13}C^{18}O$). Two isotope-sensitive modes have been located at 500 and 574 cm⁻¹. The former exhibits a monotonous isotope shift with increasing CO mass, whereas the latter displays a zigzag shift pattern. Therefore, we assign the one at 500 cm⁻¹ to the ν[Fe(II)—CO] stretching and the one at 574 cm⁻¹ to the δ[Fe(II)—C—O] bending. These two values are indeed very similar to those found in human carbonmonoxy hemoglobin A (HbA) (507 and 578 cm⁻¹), sperm whale carbonmonoxy Mb (512 and 577 cm⁻¹), and carp carbonmonoxy Hb (508 and 576 cm⁻¹) (22). The absence of two lines of comparable intensity at ≈500 cm⁻¹ in carbonmonoxy CTT III under various conditions that are known to alter the population ratio of the two species differing in heme-rotational orientation (8, 19) is interpreted to mean that the ν[Fe(II)—CO] stretching frequencies for the two components are the same at 500 cm⁻¹. The lowering of the pH value from 7.2 (Fig. 2) to 5.6 produces little change (within ±2 cm⁻¹) in ν[Fe(II)—CO].

The bound C—O stretching vibration, ν(C—O), is detected at 1960 cm⁻¹, which shifts to 1918 ($^{13}C^{16}O$), 1918 ($^{12}C^{18}O$), and 1875 cm⁻¹ ($^{13}C^{18}O$) (Fig. 3). The infrared-detected C—O stretching frequency in carbonmonoxy CTT III was reported at 1963.8 cm⁻¹ (32).

DISCUSSION

Application of Badger's Rule for the Fe—C Bond in Carbonmonoxy Heme Model Systems. The so-called Badger's Rule, which relates the equilibrium bond length (r_e) and

harmonic bond-stretching force constant (k) has the general expression (33):

$$r_e = d_{ij} + (a_{ij} - d_{ij}) k^{-1/3}, \quad [1]$$

where a_{ij} and d_{ij} are empirical constants for a pair of atoms from rows i and j in the periodic table. To determine the values of a_{ij} and d_{ij} for the (Fe,C) pair of carbonmonoxy heme systems, one needs to know at least two force constants for two different Fe—C bond lengths. Fortunately, high-precision x-ray structural data are available for Fe(II)-TPP-Py-CO (16) and Fe(II)-deut-H₄furan-CO (34). The bond-stretching force constants can be determined on the basis of ν(Fe—CO)s and normal coordinate calculations. In our approach, we first estimate the force constant that corresponds to the Fe—C bond length of 1.77(2) Å in Fe(II)-TPP-Py-CO (16). We have detected the (νFe—CO) stretching mode of this heme complex at 484 cm⁻¹, and the ν(C—O) stretching mode at 1976 cm⁻¹. The bending force constant for the Fe—C—O grouping does not affect the ν(Fe—CO) frequency if the Fe—C—O grouping is linear and perpendicular to the heme (21, 23). Although we have not observed the δ(Fe—C—O) frequency in Fe(II)-TPP-Py-CO, we used a bending force constant that corresponds to a δ(Fe—C—O) frequency close to 574 cm⁻¹ observed for the slightly distorted Fe—C—O grouping of carbonmonoxy Fe(II)SP-15 (N-MeIm) (23). Normal coordinate analysis based on the imidazole(Im)-Fe—C—O model, similar to that used in ref. 22, indicates that a force constant of 2.50 mdyne/Å is appropriate for the Fe—C bond in Fe(II)-TPP-Py-CO or Fe(II)-TPP-Im-CO. The replacement of pyridine by imidazole produces no appreciable change (i.e., within ±2 cm⁻¹) in ν[Fe(II)—CO]. The structural parameters used in our calculations are as follows: r(Fe—Im) = 2.10 Å; r(Fe—C) = 1.77 Å; r(C—O) = 1.12 Å; ϕ(Im—Fe—C) = 180°; and θ(Fe—C—O) = 180°. Imidazole was treated as a single dynamic unit with a mass of 68 amu. The Urey–Bradley force field was used for the potential function, and the force constants used were transferred from those used in ref. 22 with slight adjustments for best fit. These force constants (in mdyne/Å) are as follows: K(Fe-Im) = 1.33; K(Fe—C) = 2.50;

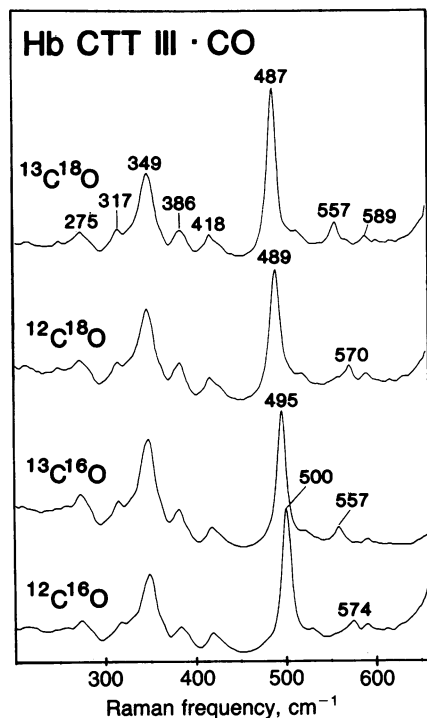FIG. 2. CO isotope effects on resonance Raman spectrum (200–650 cm⁻¹) of carbonmonoxy CTT III. λ = 406.7 nm; 70 μM in 50 mM Tris·HCl (pH 7.2). Other conditions are the same as in Fig. 1.

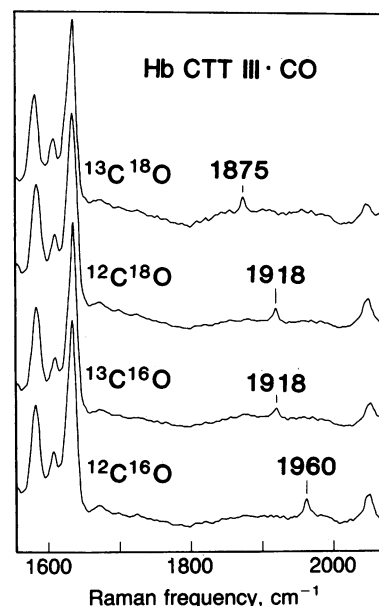FIG. 3. CO isotope effects on resonance Raman spectrum (1550–2100 cm⁻¹) of carbonmonoxy CTT III. Experimental conditions are the same as in Fig. 2 except for the delay, 5000 (152 sec).

K(C—O) = 16.3; H(Im-Fe—C) = 0.57; H(Fe—C—O) = 0.79. Stretching–stretching interaction force constants between two adjacent bonds are: F[(Im-Fe) − (Fe—C)] = 0.10 mdyne/Å and F[(Fe—C) − (C—O)] = 1.2 mdyne/Å. The seven normal modes produced by these force constants are as follows: ν(Fe—CO) = 484 cm^{-1}; ν(Fe-Im) = 240 cm^{-1}; ν(C—O) = 1976 cm^{-1}; δ_1(Im-Fe—C) = 221 cm^{-1}; δ_2(Im-Fe—C) = 221 cm^{-1}; δ_1(Fe—C—O) = 560 cm^{-1}; and δ_2(Fe—C—O) = 560 cm^{-1}, with the latter two sets being degenerate. Although experimentally the vibrations such as ν(Fe-Im), δ(Im-Fe—C), and δ(Fe—C—O) have not been assigned, we feel that these values are reasonable in view of resonance Raman data from related heme complexes (35). Here our primary concern is the estimation of the Fe—C bond stretching force constant, which corresponds to the ν(Fe—CO) frequency at 484 cm^{-1}. Other force constants within reasonable limits do not significantly affect the ν(Fe—CO) frequency. Thus, r_e = 1.77 Å for Fe(II)-TPP-Py-CO corresponds to k = 2.50 mdyne/Å.

The second force constant (k') for the Fe—C bond in Fe(II)-deut-H$_4$furan-CO can then be approximated by

$$\nu'/\nu = \sqrt{k'/k} \qquad [2]$$

Here we assume that the reduced mass for stretching the Fe—C bond is the same between Fe(II)-TPP-Py-CO and Fe(II)-deut-H$_4$furan-CO. It has been found that the ν[Fe(II)—CO] frequencies for Fe(II)-TPP-Py-CO and Fe(II)-TPP-Py-d$_5$-CO are the same (unpublished results). Thus, the small difference in the mass between Py and H$_4$furan should not affect the reduced mass. We have observed the ν(Fe—CO) frequency in Fe(II)-deut-H$_4$furan-CO at 530 cm^{-1}. Therefore, we obtain k' = 3.00 mdyne/Å, which corresponds to the r_e = 1.706(5) Å for Fe(II)-deut-H$_4$furan-CO (34). The values of a_{ij} and d_{ij} are then determined from Eq. 1: a_{ij} = 2.13 Å and d_{ij} = 0.75 Å, which now establishes the Badger's rule for the Fe—C bond as r_e = 0.75 + 1.38 $k^{-1/3}$. These Badger's constants are calculated using x-ray crystallographic data. The ν(Fe—CO) frequency for crystals of Fe(II)-TPP-Py-CO, prepared as described in ref. 16, is identical (within ±1 cm^{-1}) to that observed in solution (unpublished results). Therefore, we assume that the ν(Fe—CO) of Fe(II)-deut-H$_4$furan-CO in crystals is very close to the 530 cm^{-1} value obtained in solution.

The Influence of the Fe—C—O Bond Angle (θ) on ν[Fe(II)—CO] Frequency. The variations of ν[Fe(II)—CO] as a function of the angle (θ) of the Fe—C—O grouping, without changes in force constants, are determined using the normal coordinate analysis described above. With increasing bond angle the ν[Fe(II)—CO] frequency decreases (Fig. 4), presumably due to the increase in the effective mass of CO for the stretching of the Fe—C bond. Our calculations show the percentage of potential energy derived from the Fe—C coordinate ranges from 92% ($\theta \approx$ 180° and 110°) to 65% ($\theta \approx$ 145°). Mixing between the stretching and bending is quite appreciable at θ near 145°.

The Expected ν[Fe(II)—CO] Frequency in Carbonmonoxy CTT III Based on X-Ray Structural Data. The x-ray crystallographic structure of carbonmonoxy CTT III has been determined at 1.4-Å resolution (18). The Fe—C bond length was reported as 2.4 Å, which is unusually large compared to the values found in carbonmonoxy human HbA (1.80 Å) (36) and the heme model complex Fe(II)-TPP-Py-CO (1.77 Å) (34). Other relevant structural parameters include the Fe—C—O bond angle of 161° ± 5° and a tilt angle of 8°. With these structural data, the expected ν[Fe(II)—CO] frequency can now be estimated. The starting point in the estimation scheme (Fig. 5) is the Raman structural data of Fe(II)-TPP-Py-CO. Since the replacement of pyridine by imidazole
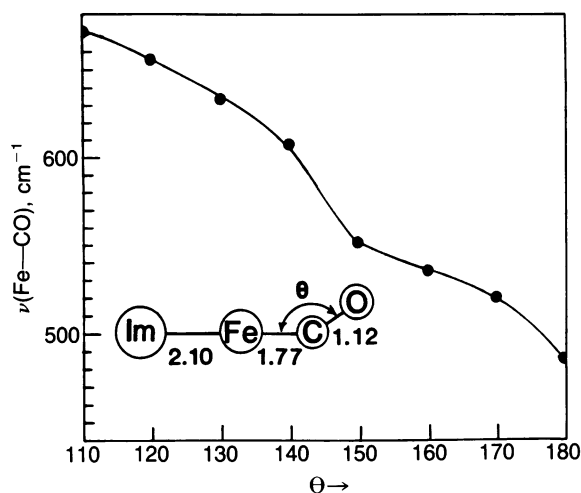

FIG. 4.   Variation of ν(Fe—CO) as a function of Fe—C—O (θ) angle. No changes in force constants.

makes no appreciable difference in ν[Fe(II)—CO], we prefer to use Fe(II)-TPP-imidazole-CO in our discussion. Step 1 involves a change in the Fe—C—O angle from 180° to 161° without changes in the force constants and other structural parameters. Such a bond angle change would increase the ν[Fe(II)—CO] frequency from 484 to 535 cm^{-1} (Fig. 4). In step 2 the Fe—C bond length is increased from 1.77 to 2.4 Å, resulting in a decrease in the Fe—C force constant (k) from 2.50 to 0.59 mdyne/Å. This change in k decreases the ν(Fe—CO) frequency to 535 (0.59/2.50)$^{1/2}$ or 260 cm^{-1}. The final step 3 is a tilting of the Fe—C bond from the heme normal by 8°. Recent studies in carbonmonoxy "strapped hemes" by Yu *et al.* (23) revealed that in the case with the most severe tilting of CO, the ν(Fe—CO) frequency increases by only 19 cm^{-1}. Thus, the upper limit for the ν[Fe(II)—CO] frequency expected on the basis of x-ray structural data is 279 cm^{-1}, which differs greatly from the observed 500 cm^{-1}. It is noted that the most important contribution in this scheme is the force-constant correction (step 2). It provides sufficient evidence itself that the x-ray data must be in error.

Geometry of the Fe—C—O Grouping Deduced from Resonance Raman Data. Raman data can be obtained with ease from model compounds and hemoproteins in both crystal and solution. Therefore, it would be of interest to have some methodology for deducing ligand geometry. We make a first attempt here by estimating the Fe—C—O geometry of carbonmonoxy CTT III consistent with our resonance Raman data for this heme protein. This by no means has the same precision as an x-ray-determined structure; however, it is possible to place an upper limit on the Fe—C bond length. The procedure, similar to the scheme used in estimating the ν(Fe—CO) frequency begins with the spectral and structural data of the model Fe(II)-TPP-Im-CO. By using an equation
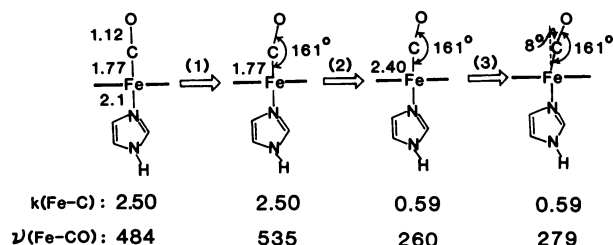

FIG. 5.   Scheme for the prediction of ν(Fe—CO) in CTT III CO using the x-ray data of Steigemann and Weber (18) (Fe—C bond length = 2.4 Å, $\angle$Fe—C—O = 161° and tilt angle = 8°).

derived previously (23), isotope shifts of ν[Fe(II)—CO] and ν(C—O) can estimate the Fe—C—O bond angle. This angle (θ) was found to be 169 ± 5°, which is somewhat larger than the 161 ± 5° value obtained by Steigemann and Weber in their x-ray crystallographic studies (18). With this geometric arrangement and the observed ν(Fe—CO) frequency of 500 cm^{-1}, Badger's rule predicts an Fe—C bond length of 1.80 Å.

It is still not possible to estimate the tilt angle; however, Yu *et al.* (23) suggested that the intensity ratio between the δ(Fe—C—O) bending and the ν(Fe—CO) stretching is indicative of the degree of tilting. However, if we assume that the tilting is the most severe, as has been observed in the model system (23), the upper limit for the Fe—C bond length is 1.82 Å estimated according to Badger's rule. Thus, the Raman data predict a final structure where the CO is tilted, the Fe—C—O group is bent to ≈169°, and the Fe—C distance lies within the range of models and other heme proteins. Therefore, it is concluded that the Fe—C bond length should not be >1.82 Å in carbonmonoxy CTT III, a result largely different from the crystallographic results.

Comparison of Fe—C Bond Lengths in Carbonmonoxy and Cyanomet CTT III. The ν[Fe(III)—CN$^-$] frequency (at 453 cm^{-1}) is 47 cm^{-1} lower than the ν[Fe(II)—CO] frequency at 500 cm^{-1} (cf. Figs. 1 and 2). If the Badger's rule for the Fe—CO bond is a good approximation for the Fe—CN bond, the much lower ν[Fe(III)—CN] frequency at 453 cm^{-1} suggests that the Fe—CN bond is longer than the Fe—CO bond. However, this is contrary to the x-ray data by Steigemann and Weber (18), who reported that the Fe—CN bond (2.2 Å) in cyanomet CTT III is shorter than the Fe—CO bond (2.4 Å) in carbonmonoxy CTT III.

Recently, Scheidt *et al.* (17) reported the Fe—CN bond distance of 1.908(4) Å in cyano(pyridine)(*meso*-tetraphenylporphinato) iron(III), Fe(III)-TPP-Py-CN$^-$, which is 0.138 Å longer than the 1.77 Å value for the Fe—CO bond distance in Fe(II)-Py-TPP-CO. Can the protein reverse the order of these two relative bond distances? Resonance Raman studies of Fe(III)-TPP-Py-CN$^-$ in benzene (unpublished results) detected the ν[Fe(III)—CN$^-$] frequency at 452 cm^{-1}, very similar to the 453 cm^{-1} in cyanomet CTT III and the 455 cm^{-1} in cyanomet carp Hb (22). This strongly suggests that the Fe—CN bond lengths in cyano-met hemoglobins must be very close to the 1.908 Å value. Since the upper limit for the Fe—CO bond length in carbonmonoxy CTT III is 1.82 Å, the Fe—CN bond may indeed be longer than the Fe—CO bond in the CTT III system, in disagreement with the x-ray crystallographic results (18). It is interesting that the Fe—C bond in Fe(III)-TPP-Py-CN$^-$ (or cyanomet CTT III) is longer than that in the Fe(II)-TPP-Py-CO (or carbonmonoxy CTT III) despite the charge interaction between Fe(III) and CN$^-$. The lone pair electrons of both CN$^-$ and CO ligands coordinate to the d$_{z^2}$(Fe) orbital to form a σ bond. However, in carbonmonoxy complexes, there may be a greater π-bonding between d$_\pi$(Fe) and π^*(CO). Although we do not believe the Fe(III)CO$^-$ formulation, there may be some partially negative charge on the CO ligand and some partially positive charge on the heme iron. In any event, the shorter Fe—C bond in carbonmonoxy complexes seems to be caused by the substantial π-bonding interaction between d$_\pi$(Fe) and π^*(CO).

1. Gersonde, K. (1983) in *Biological Oxidations*, 34th Colloquium-Mosbach 1983, eds. Sund, H. & Ullrich, V. (Springer, Berlin), pp. 170–188.
2. Gersonde, K., Sick, H., Wollmer, A. & Buse, G. (1972) *Eur. J. Biochem.* **25**, 181–189.
3. Trittelvitz, E., Sick, H., Gersonde, K. & Ruterjans, H. (1973) *Eur. J. Biochem.* **35**, 122–125.
4. Overkamp, M., Twilfer, H. & Gersonde, K. (1976) *Z. Naturforsch. C.* **31**, 524–533.
5. Gersonde, K., Twilfer, H. & Overkamp, M. (1982) *Biophys. Struct. Mech.* **8**, 189–211.
6. Christahl, M. & Gersonde, K. (1982) *Biophys. Struct. Mech.* **8**, 271–288.
7. Sick, H., Gersonde, K., Thompson, J. C., Maurer, W., Haar, W. & Ruterjans, H. (1972) *Eur. J. Biochem.* **29**, 217–223.
8. LaMar, G. N., Overkamp, M., Sick, H. & Gersonde, K. (1978) *Biochemistry* **17**, 352–361.
9. LaMar, G. N., Viscio, D. B., Gersonde, K. & Sick, H. (1978) *Biochemistry* **17**, 361–367.
10. Ribbing, W. & Ruterjans, H. (1980) *Eur. J. Biochem.* **108**, 89–102.
11. Krümpelmann, D., Ribbing, W. & Ruterjans, H. (1980) *Eur. J. Biochem.* **108**, 103–109.
12. LaMar, G. N., Anderson, R. R., Budd, D. L., Smith, K. M., Langry, K. C., Gersonde, K. & Sick, H. (1981) *Biochemistry* **20**, 4429–4436.
13. Sick, H. & Gersonde, K. (1974) *Eur. J. Biochem.* **45**, 313–320.
14. Steffens, G., Buse, G. & Wollmer, A. (1977) *Eur. J. Biochem.* **72**, 201–206.
15. Hoard, J. L. (1975) in *Porphyrins and Metalloporphyrins*, ed. Smith, K. M. (Elsevier, Amsterdam), pp. 317–380.
16. Peng, S. & Ibers, J. A. (1976) *J. Am. Chem. Soc.* **98**, 8032–8036.
17. Scheidt, W. R., Lee, Y. J., Luangdilok, W., Haller, K. J., Anzai, K. & Hatano, K. (1983) *Inorg. Chem.* **22**, 1516–1522.
18. Steigemann, W. & Weber, E. (1979) *J. Mol. Biol.* **127**, 309–338.
19. LaMar, G. N., Smith, K. M., Gersonde, K., Sick, H. & Overkamp, M. (1980) *J. Biol. Chem.* **255**, 66–70.
20. Sick, H., Gersonde, K. & LaMar, G. N. (1980) *Hoppe Seyler's Z. Physiol. Chem.* **361**, 333–334.
21. Yu, N.-T. (1984) *Methods Enzymol.* **79**, in press.
22. Tsubaki, M., Srivastava, R. B. & Yu, N.-T. (1982) *Biochemistry* **21**, 1132–1140.
23. Yu, N.-T., Kerr, E. A., Ward, B. & Chang, C. K. (1983) *Biochemistry* **22**, 4534–4540.
24. Kerr, E. A., Mackin, H. C. & Yu, N.-T. (1983) *Biochemistry* **22**, 4373–4379.
25. Benko, B. & Yu, N.-T. (1983) *Proc. Natl. Acad. Sci. USA* **80**, 7042–7046.
26. LaMar, G. N., Anderson, R. R., Chacko, V. P. & Gersonde, K. (1983) *Eur. J. Biochem.* **136**, 161–166.
27. Yu, N.-T. & Srivastava, R. B. (1980) *J. Raman Spectrosc.* **9**, 161–171.
28. Choi, S., Spiro, T. G., Langry, K. C. & Smith, K. M. (1982) *J. Am. Chem. Soc.* **104**, 4337–4344.
29. Rousseau, D. L., Ondrias, M. R., LaMar, G. N., Kong, S. B. & Smith, K. M. (1983) *J. Biol. Chem.* **258**, 1740–1746.
30. Rousseau, D. L. & Ondrias, M. R. (1983) *Annu. Rev. Biophys. Bioeng.* **12**, 357–379.
31. Henry, E. R. (1980) Dissertation (Princeton Univ., Princeton, NJ).
32. Wollmer, A., Steffens, G. & Buse, G. (1977) *Eur. J. Biochem.* **72**, 207–212.
33. Herschbach, D. R. & Laurie, V. W. (1961) *J. Chem. Phys.* **35**, 458–463.
34. Scheidt, W. R., Haller, K. J., Fons, M., Mashiko, T. & Reed, C. A. (1981) *Biochemistry* **20**, 3653–3657.
35. Spiro, T. G. (1983) in *Iron Porphyrins*, eds. Lever, A. B. P. & Gray, H. B. (Addison-Wesley, Reading, MA), Part 2, pp. 89–152.
36. Baldwin, J. M. (1980) *J. Mol. Biol.* **136**, 103–128.